

Investigation of Al-Ni Alloys Deposition during Over-discharge Reaction of Na-NiCl₂ Battery

Jeongsoo Kim^{1,3}, Seung Hwan Jo^{1*}, Dae-In Park¹, Sai Bhavaraju², and Sang Ook Kang³

¹Battery R&D center, SK INNOVATION, 325 Exporo, Yuseong-gu, Daejeon 305-712, South Korea

²Ceramatec, Inc. 2425 S 900 W, Salt Lake City, UT 84119, United States of America

³Department of Advanced Materials Chemistry, Korea University, 2511 Sejong-ro, Sejong 339-700, South Korea

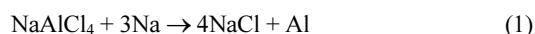
(Received February 29, 2016 : Revised March 8, 2016 : Accepted March 12, 2016)

Abstract : The over-discharging phenomena in sodium-nickel chloride batteries were investigated in relation to decomposition of molten salt electrolyte and consequent metal co-deposition. From XRD analysis, the material deposited on graphite cathode current collector was revealed to be by-product of molten salt electrolyte decomposition. In particular, the result showed that the Ni-Al alloys (Al₃Ni₂, Ni₃Al and Al₃Ni) were electrochemically deposited on graphite current collectors in line with over-discharging behaviors. It is assumed that the NiCl₂ solubility in molten salt electrolytes leads to the co-deposition of Ni-Al alloys by increasing metal deposition potential above 1.6 V (vs. Na/Na⁺). The cell tests have revealed that the composition of molten salt electrolytes modified by various additives makes a decisive influence on the over-discharging behaviors of the cells. It was revealed that NaOCN addition to molten salt electrolytes was advantageous to suppress over-discharge reactions by modifying the characteristics of molten salt electrolytes. NaOCN addition into molten salt electrolytes seems to suppress Ni solubility by maintaining basic melts. The cell using modified molten salt electrolyte with NaOCN (Cell D) showed relatively less cell degradation compared with other cells for long cycles.

Keywords : ZEBRA battery, NaSICON, molten salt electrolyte, over-discharge, metal deposition

1. Introduction

There has been tremendous interest on the sodium-metal chloride battery (Zebra battery) which utilizes a liquid sodium anode and a metal chloride cathode separated by a sodium ion conducting solid electrolyte, β''-Alumina.¹⁻⁶ The molten NaAlCl₄ impregnated into the porous cathode structure (Ni-NaCl composite) conducts Na⁺ ions between the β''-Alumina surface and reaction sites of cathode.⁷ If β''-Alumina ceramic is broken, the molten NaAlCl₄ directly contacts with liquid sodium and react as following equation.



The same reaction is also caused by cell over-

discharge below 1.6 V, which leads to the decomposition of NaAlCl₄ and the deposition of Al in cathode. Generally, Al has been considered as a quite interesting coating material because it can effectively protect the metals from corrosion.⁸⁻¹⁰ Although various techniques have been developed to produce Al alloy coating, it is not easy to produce Al alloy from aqueous electrolyte due to high hydrolysis potential. For this reason, electro-deposition has been studied as an alternative method to form Al alloy successfully.¹¹⁻¹³ Although it is well known that Al could be formed in Zebra battery cells, there is no reports treating Al deposition in the cathode current collectors of Zebra battery even without cell failure. Interestingly, Al-Ni alloy co-deposition was reported to occur in the NiCl₂/AlCl₃/EMImBr (0.03/2/1) solution at 0.3 V higher voltage¹⁴ than that of pure Al deposition.¹⁵ This could be a thought-provoking result that co-deposi-

*E-mail: shjo0829@gmail.com

tion of Ni-Al alloy can be a critical issue to be considered for the long life cycle of Zebra battery. Generally, it is well known that Ni particle growth is the main degradation factor of Zebra battery.^{7,16-18} Also, the Ni particle growth is significantly accelerated by high solubility of NiCl₂ in molten salt electrolyte. The solubility of NiCl₂ in molten salt electrolyte can be affected by various factors such as operation temperature, the composition of cathode and molten salt electrolytes, and cycling condition.¹⁹⁻²⁴

In a different aspect, high NiCl₂ solubility leads to the deposition of Ni and may cause the decomposition of NaAlCl₄ easily by increasing Al³⁺ reduction potential from 1.6 V to >2.0 V. Zhang et al.¹⁴ have suggested that the co-deposition of Al and Ni indicates the increase of NiCl₂ solubility in AlCl₃/EMImBr solution, and this can rearrange the deposition potential toward 0.3 V higher in the NiCl₂/AlCl₃/EMImBr (0.03/2/1).

In this study, we have investigated on the over-discharge behaviors of Zebra batteries with different molten salt electrolytes during formation cycles and investigated the composition of the material coated on the graphite current collectors. From the cyclic performance and over-discharge behaviors of the cells, we have discussed the possible effects of molten salts electrolytes with different composition on the long-term performance of Zebra battery affected by electrolyte decomposition and subsequent metal deposition.

2. Experimental

2.1 Preparation and characterization of molten salt electrolytes

The NaAlCl₄ based molten salts were synthesized by a self-developed procedure as follows. Initially, as received raw materials of NaCl (Sigma-Aldrich 99.5%), NaOCN (Sigma-Aldrich 99.5%) and NaI (Sigma-Aldrich 99.5%) were dried in a vacuum oven at 80°C for three days to remove residual humidity. In the case of AlCl₃ (Sigma-Aldrich, 99%, anhydrous), further purification is carried out by a sublimation method after mixing AlCl₃ and small amount of NaCl and Al shots with an argon gas at 175°C. The purified AlCl₃ was ground to

particles and moved into a Teflon container in an argon gas purged glove box with NaCl and with/without additives (NaOCN and NaI) according to the developed recipe. Finally, the container is heated at 170°C for 12 h to get homogeneous molten salts.

2.2 Cathode preparation

To prepare cathode powder, NaCl (Sigma-Aldrich, 99.5%) and Ni (Vale, type 255) powders were homogeneously mixed for 48 h in a dry atmosphere to have a Ni/NaCl molar ratio of 3/1. Fine size (<45 μm) of NaCl powder was obtained by an energetic dry ball milling at 300 rpm. The prepared cathode mixture was poured into a specially designed stainless (diameter: Φ 19) steel mold and weakly tapped for seconds followed by pressing under 48 MPa to achieve pressed cathodes with 165 mAh capacity. The prepared cathode disks were reserved in the glove box until it is used for cell test.

2.3 Full cell test

NaSICON (Na_{1+x}Zr₂Si_xP_{3-x}O₁₂) disks manufactured by Ceramatec Ltd. (Salt lake city, USA) were used as a separator. The NaSICON disks have 1 mm thickness and Φ 19 diameter. With different compositions of molten salt electrolytes, we have conducted full cell tests to verify how each cell shows over-discharge behavior during formation cycles. The each disk-type cathode connected with graphite current collectors was placed at one side of the NaSICON disk with the minimum amount of sodium metal on opposite side. After being assembled and sealed with Teflon O-rings and bolt/nut fastening, the cells with four kinds of molten salt electrolytes were tested at 160°C (A, B) and 170°C (C, D) using a WonAtech (WBCS 3000; WonAtech, Seoul, South Korea) charge-discharge system. The formation step was conducted at current density of 6 mA/cm² (0.1C) for 3 cycles. Subsequently, the degradation of the cells was compared at 12 mA/cm² (0.2C). In addition, X-ray diffraction (D/MAX-IIIC X-ray diffractometer, Rigaku, Tokyo, Japan) was conducted to figure out the materials formed on cathode current collector of Cell A after cycling test. Before cell disassembly, the cell was fully discharged.

3. Results and discussion

Table 1 displays the cell code, molten salt composition and test condition of the cells. Since previous studies on Zebra battery indicate that NiCl_2 solubility in NaAlCl_4 affects on degradation behavior of cells, we tried to develop unique molten salt electrolyte composition by testing various compositions. Fig. 1(a) shows the schematic configuration of the cells adapted in this study. The background of this work is that the specific material tends to deposit on the surface of graphite current collectors as shown in Fig. 1(b), when the cells experienced over-discharge phenomena. The over-discharge of the cells means that the coulombic efficiency during cycles exceeds 100%. To reveal the phases of coated materials, X-ray diffraction was carried out with Cell A as described in Fig. 2. Although the graphite current collectors are immersed in molten NaAlCl_4 during cell tests, the coated material was revealed to contain Ni-Al alloys with NaAlCl_4 and some other known materials. This is a quite interesting result to imply that NaAlCl_4 molten salt could decompose partially during charge and discharge reaction cycles. It has been generally known that the decomposition reaction of NaAlCl_4 occurs when the voltage goes down below 1.6 V as described in the introduction by equation (1).¹⁵⁾

The XRD result confirms that the decomposition of molten salt electrolytes since it contains NaCl and NaAlCl_4 as main components. However, the thought-provoking feature unsolved is why some Ni-Al alloys such as Al_3Ni_2 , Ni_3Al and Al_3Ni are coated on the current collectors. This phenomenon is supported by the results reported by Zhang et al.¹⁴⁾ The report explains that the co-deposition of Al-Ni alloys in $\text{AlCl}_3/\text{EMImBr}$ solution due to NiCl_2 solubility in the solution rearranges the Al

deposition potential 0.3 V higher in the $\text{NiCl}_2/\text{AlCl}_3/\text{EMImBr}$ (0.03/2/1) at room temperature. In Zebra battery chemistry, Al deposition potential is known to be 1.6 V vs. Na/Na^+ reaction at 300°C. However, when NiCl_2 in cathode is dissolved in the molten

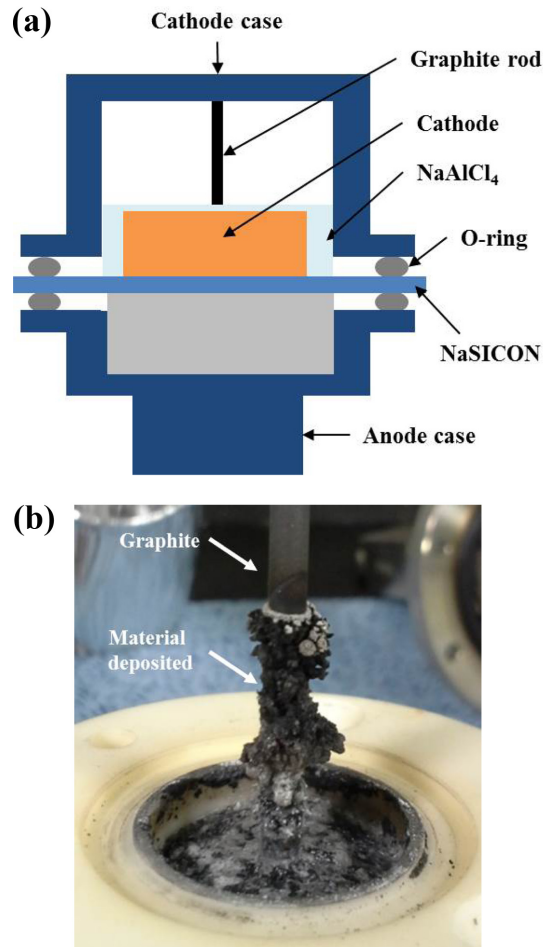


Fig. 1. (a) Schematic of cell configuration and (b) image of deposited material on graphite current collector from Cell A.

Table 1. Cell code, molten salt composition and test condition of the cells

Cell code	Molten salt electrolyte		Temperature (°C)	Voltage range (V)
	Component	Mole ratio		
A	$\text{NaCl}/\text{Na}/\text{AlCl}_3$	0.9/0.1/1	160	2.9~2.2
B	$\text{NaCl}/\text{Na}/\text{AlCl}_3$	0.7/0.3/1	160	2.9~2.2
C	$\text{NaCl}/\text{AlCl}_3$	1/1	170	2.9~2.2
D	$\text{NaCl}/\text{NaOCN}/\text{AlCl}_3$	0.95/0.05/1	170	2.9~2.2

salt electrolyte, the Al deposition potential seems to increase toward Ni deposition potential (2.6 V) resulting in the formation of Ni-Al alloys. The co-deposition potential of Ni-Al alloys seems to proportionally move upward as the NiCl_2 solubility in molten salt electrolytes increases.

The charge and discharge patterns of the cells are compared in Fig. 3. Although four cells were operated above 1.6 V, all of them exhibited over-discharging behaviors noticeably at 1st formation cycle, which show the higher capacity utilizations at discharge reactions than those at charge reactions. However, the extent of over-discharge reactions tends to differ depending on the composition of molten salt electrolytes. From the summarized data of capacity utilizations and coulombic efficiencies of the cells in Fig. 4(a), the noticeably high coulombic efficiencies were observed for the cells A (143%) and B (154%) using molten salt electrolytes that NaCl is partially substituted by NaI. The cell using reference NaAlCl_4 electrolyte (Cell C) also exhibited high coulombic efficiencies of 130% at 1st cycle. In the previous report,²⁴⁾ it has been noted that the NaAlCl_4 molten salt is designed to

have excess amount of NaCl (the molar ratio of $\text{NaCl}:\text{AlCl}_3 = 0.51:0.49$) to prevent the formation of Lewis-acidic melts which increase the Ni solubility.²³⁾ As a result, the high coulombic efficiency of the cell C using stoichiometric NaAlCl_4 at 1st formation cycle could be attributable to the formation of Lewis-acidic melts. Therefore the relatively severe over-discharges for cells A and B using modified molten salt electrolytes with NaI imply that NiCl_2 is likely to dissolve easily in the molten salt electrolytes containing NaI because I^- ions are more likely to dissolve than Cl^- ions due to their larger anion size.

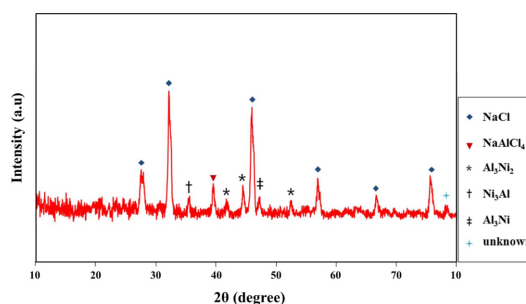


Fig. 2. XRD analysis of the material deposited on graphite current collector from Cell A.

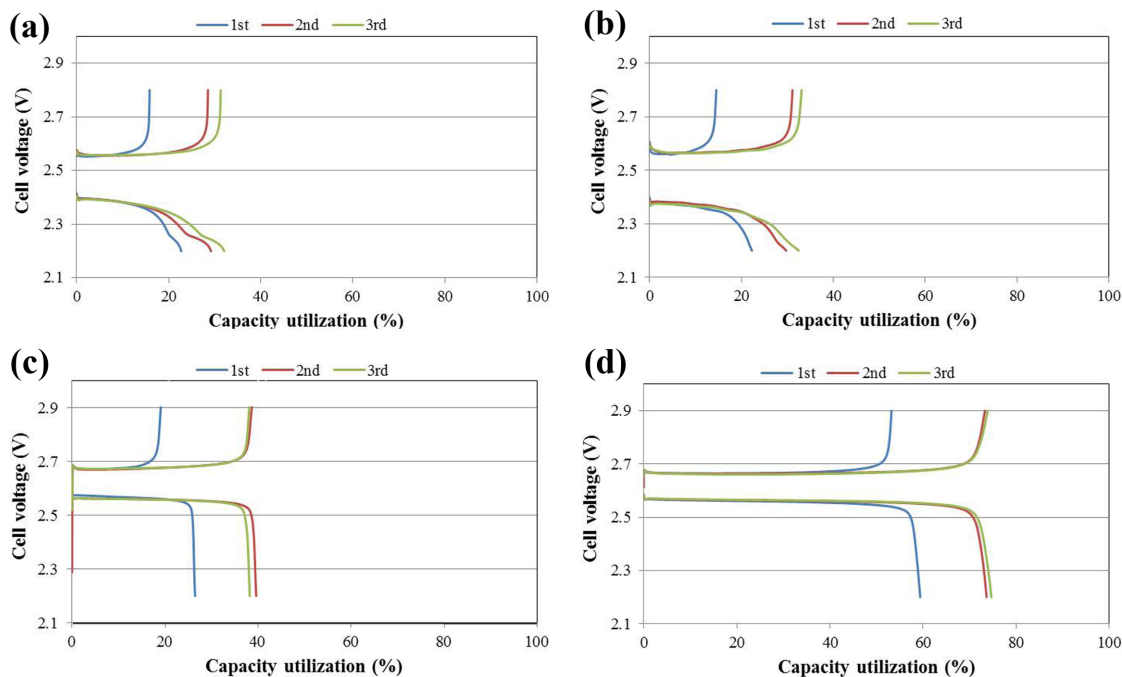


Fig. 3. Formation data of (a) cell A, (b) cell B at 160°C and (c) cell C, (d) cell D at 170°C.

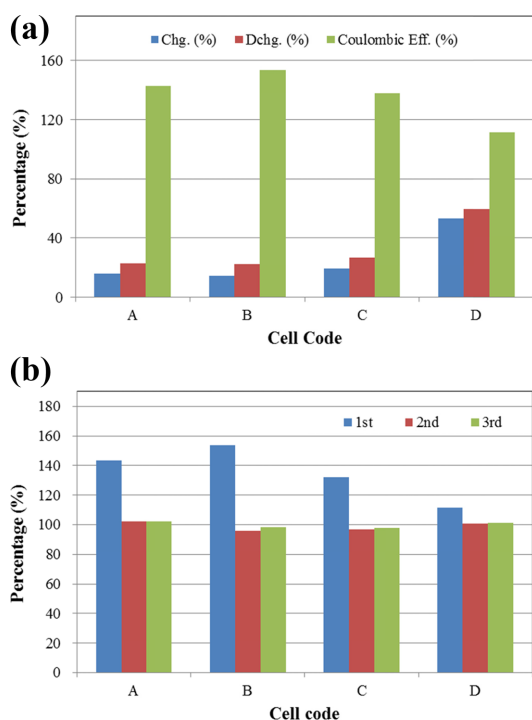


Fig. 4. (a) Charge & discharge utilization and coulombic efficiency of the cells at 1st formation cycle, (b) coulombic efficiency of the cells at 1st, 2nd and 3rd cycle.

However, the coulombic efficiencies of the cells are at 2nd and 3rd cycles are around 100%, which convinces that over-discharging behaviors at 1st formation cycle seem to disappear from 2nd cycle as described in Fig. 4(a). This infers that the molten salt electrolytes return to basic melts from 2nd cycle since the AlCl_3 depletes to form Ni-Al alloys and the molten salt electrolytes maintain basic melts with less AlCl_3 .

As an alternative to keep the molten salts electrolyte as basic melts,²³⁾ NaOCN was partially substituted to NaCl. Interestingly, the cell D using this electrolyte composition ($\text{NaCl}/\text{NaOCN}/\text{AlCl}_3 = 0.95/0.05/1$) exhibited relatively lower coulombic efficiency (112%) at 1st cycle. In addition, the higher discharge capacity utilization (59%) was obtained for the cell D compared with that of cell C (36%). This result indicates that NaOCN is effective to increase capacity utilization of Zebra battery.

In addition, it seems that NaOCN is helpful to weaken over-discharging behavior at 1st formation cycle as shown in Fig. 4(a). This probably supports

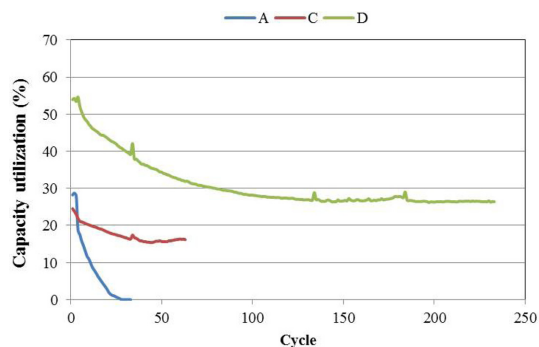


Fig. 5. Capacity retention behaviors of the cells with different molten salt electrolytes.

the positive effects of NaOCN as an additive to reduce NiCl_2 solubility by keeping the molten salts as basic melts, which results in the decrease of Al-Ni co-deposition potential to suppress the co-deposition of Al-Ni alloys at 1st cycle. As a result, the modification of molten salt electrolytes with various additives may be advantageous to lower the NiCl_2 solubility and ultimately prevent over-discharge reactions. Since the Ni solubility is intensely related to Ni particle growth which causes rapid cell degradation of Zebra battery,^{22,24)} the long-term performance of the cells A, C, and D were compared at 12 mA/cm² (0.2C) in Fig. 5. Although the cell D also exhibited capacity degradation similarly to other cells, it is obvious that the cell D maintained higher capacity utilization than other cells due to the modified molten salt electrolyte with NaOCN for long cycles. Since the degradation of Zebra battery is also attributable to other various parameters such as operation temperature, the composition of cathode and battery cycling conditions other than the composition of molten salt electrolytes, further investigation would be necessary to reveal the effects of NaOCN in molten salt electrolytes to lower Ni solubility and ensure less cell degradation.

4. Conclusion

Electrochemical co-deposition of Ni-Al alloys was observed for Zebra battery linked to over-discharging behaviors at 1st formation cycle. X-ray diffraction result confirmed the decomposition of NaAlCl_4 molten salt to NaCl and Ni-Al alloys (Al_3Ni_2 ,

Ni₃Al and Al₃Ni). It seems that the NiCl₂ dissolution in molten salt electrolytes leads to the co-deposition of Ni-Al alloys by raising metal deposition potential above 1.6 V (vs. Na/Na⁺). From the cell tests with different molten salt electrolytes, it has been revealed that the composition of molten salt electrolytes modified by various additives can be a decisive factor to cause over-discharging behaviors of the cells. The cell tests proved that NaOCN is an effective additive to suppress over-discharge reactions by modifying the characteristics of molten salt electrolytes. The D cell using modified molten salt electrolyte with NaOCN showed relatively stable cell performance for 240 cycles.

Acknowledgments

The authors acknowledge a grant-in-aid from SK innovation supported by Ceramatec, Inc. for NaSiCON development.

References

1. J. Coetzer, Ext. Abstr., 170th Meet. Electrochemical Society, San Diego, CA, USA, Oct 1986. Abstr. No. 762.
2. R. C. Galloway, Ext. Abstr., 172nd Meet. Electrochemical Society, Honolulu, HI, USA, Oct. 1987 Abstr. No. 159.
3. Coetzer, *J. Power Sources*, **18**, 377 (1986).
4. R. C. Galloway, *J. Electrochemical Soc.*, **134**, 256 (1987).
5. M. Sudoh and J. Newman, *J. Electrochem. Soc.*, **137**, 876 (1990).
6. J. Coetzer, G. D. Wald, and S. W. Orchard, *J. Appl. Electrochem.*, **23**, 790 (1993).
7. C.-D. Dustman, *J. Power Sources*, **127**, 85 (2004).
8. S. Caporali, A. Fossati, and U. Bardi, *Corros. Sci.* **52**, 235 (2010).
9. L. Barci, U. Bardi, S. Caporali, M. Fantini, and A. Scivani, *Prog. Org. Coat.*, **67**, 146 (2010).
10. G. Yue, S. Zhang, Y. Zhu, X. Lu, S. Li, and Z. Li, *AIChE J.*, **55**, 783 (2009).
11. S. J. Pan, W. T. Tsai, and I. W. Sun, *Electrochem. Solid-State Lett.* **13**, D69 (2010).
12. D. Pradhan and R. G. Reddy, *Electrochim. Acta*, **54**, 1874 (2009).
13. S. S. V. Tatiparti, F. Ebrahimi, *J. Electrochem. Soc.*, **155**, D363 (2008).
14. L. Zhang, X. Yu, Z. Ge, Y. Dong, and D. Li, *Appl. Mech. Mater.* **121**, 65 (2012).
15. X. Lu, G. Xia, J. P. Lemmon, and Z. Yang, *J. Power Sources*, **195**, 2431 (2010).
16. J. L. Sudworth, *J. Power Sources*, **100**, 149 (2001).
17. J. L. Sudworth, *J. Power Sources*, **51**, 105 (1994).
18. K. B. Hueso, M. Armand, and T. Rojo, *Energy Environ. Sci.* **6**, 734 (2013).
19. G. Li, X. Lu, C. A. Coyle, J. Y. Kim, J. P. Lemmon, V. L. Sprenkle, and Z. Yang, *J. Power Sources*, **220**, 193 (2012).
20. M. Hosseinifar and A. Petric, *J. Power Sources*, **206**, 402 (2012).
21. J. Prakash, L. Redey, D. R. Vissers, and J. DeGruson, *J. Appl. Electrochem.* **30**, 1229 (2000).
22. J. Prakash, L. Redey, and D. R. Vissers, *J. Electrochem. Soc.*, **147**, 502 (2000).
23. B. V. Ratnakumar, S. Surampud, G. Halpert, *J. Power Sources*, **48**, 349 (1994).
24. G. Li, X. Lu, J. Y. Kim, J. P. Lemmon, and V. L. Sprenkle, *J. Mater. Chem., A* **1**, 14935 (2013).